ICAIC
International Conference for Academia and Industry Co-operation
20/11/2023 – 24/11/2023
São Luís - Maranhão - Brasil
IMMSEM
International Meeting in Materials Science and Engineering of Maranhão

PURE AND Fe-MODIFIED $B_{12}N_{12}$ NANOCAGE AS SENSOR FOR N_2O GAS: A DFT STUDY

Natanael S. Sousa[1*], Welington Lobato[1], Francivaldo S. Silva[1], Jaldyr J. G. V. Junior[1]

1 - Programa de Pós Graduação em Química - PPGQUIM, Universidade Federal do Maranhão (UFMA), 65080-805, São Luís, MA, Brazil.

natanael.sousa@discente.ufma.br

ABSTRACT

Nitrous oxide (N_2O) role as a greenhouse gas and can also contribute to the depletion of the ozone layer. To contribute to efficient detection of N_2O in the atmosphere, chemical sensors based on BN nanocages can be employed. In this context, DFT-D3 level calculations using B3LYP and 6-31G(d,p) basis set were performed in this work to investigate the geometric, electrical and energetic parameters, as well the electronic sensitivity of the adsorption of N_2O gas on pristine and Fe-modified $B_{12}N_{12}$ nanocages. The electronic sensitivity of the systems to N_2O adsorption was analyzed and Fe@b_{64} showed greater sensitivity (ΔE_{gap} = 32 %) compared to the others. The results shows that N_2O weakly adsorbs on $B_{12}N_{12}$ cage (E_{ads} = -0.14 eV). On the other hand, N_2O moderately interacts with Fe@b_{64} nanocage (E_{ads} = -0.70 eV) and presents a good recovery time (τ = 6.7 ms). In summary, the Fe@b_{64} nanocage can be used as a conductometric material for the detection of N_2O molecule gas.

Keywords: *$B_{12}N_{12}$, sensor, N_2O, Nitrous oxide, nanocages.*

INTRODUCTION

Nitrous oxide (N_2O) is a gas that has worrying environmental effects and has toxic properties that can cause harm to human health. In addition to its role as a greenhouse gas, N_2O can also contribute to the depletion of the ozone layer. Some human activities are positive for the emission of N_2O into the atmosphere, such as the use of nitrogen fertilizers, burning of fossil fuels and industrial processes. However, the effects of N_2O in the atmosphere can be mitigated through more efficient agricultural processes, responsible use of fertilizers and advanced technology for detecting the N_2O toxic gas.

Adsorption or sensing of small (toxic) gas molecules on proper semiconductors is of prime importance in environmental monitoring [1]. In the last years several studies revealed the promising utility of graphene as the best adsorbent for gas molecules [2,3]. However, the zero-band gap and weak binding (physisorption) of graphene with incident gases including NH_3, NO_2, N_2, H_2, CO, CO_2 highlighted its limitations in chemisorption applications [4-6]. Entretanto, other fullerene-like cages have also proved to be useful in sensors [7-9]. Among them, boron nitride nanocages $(BN)_n$ have excellent properties such as heat resistance in the air, large gap, structural stability and oxidation resistance [10,11].

In this theoretical work, Fowler et al. [12] presents the $B_{12}N_{12}$ is magic stable BN nanocages, and other studies demonstrate that this nanocage consist of six tetragonal and eight hexagonal rings [13–15] and Oku et al. [16] have synthesized these magic cages by using laser

desorption time-of flight mass spectrometry. Additionally, the sensitivity and selectivity of BN can be modified with transition metal atoms, as presented in literature [17-20] and recently, the theoretical studies demonstrated that the $B_{12}N_{12}$ nanocage can be used as chemical sensors for CO, NO and NH_3[21], CO [22,23], NO and C_2H_2 [24], NO, NO_2, N_2O, NH_3 [25], N_2O [26], SO_2, O_3 [27], CO, CO_2, H_2O and NH_3 [28]. Those results show the $B_{12}N_{12}$ potential to be used as chemical material to detect many toxic gas. So, in this we studied the sensibility of N_2O gas adsorption on Fe-modified $B_{12}N_{12}$ nanocage for a chemo sensor material application.

MATERIALS AND METHODS

DFT calculations were developed using ORCA 5.0[28]. Isolated $B_{12}N_{12}$ and nanocages built by Fe-modified were relaxed using the B3LYP-D3[29-30] functional and the 6-31G(d,p) basis set, as well as frequency analysis used for confirmation of global minima of the optimized structures. Modification of the $B_{12}N_{12}$ with Fe resulted in five optimized structures [31]: Doped ($FeB_{11}N_{12}$ and $B_{12}N_{11}Fe$), for replacement of a B and a N by a Fe, respectively; Decorated ($Fe@b_{64}$ and $Fe@b_{66}$), with a Fe atom positioned above a bond between the tetragonal and hexagonal rings (b_{64}) and above a bond between two hexagonal rings (b_{66}), respectively and Encapsulated ($Fe@B_{12}N_{12}$), in which an Fe atom is positioned inside the cage.

The structures were calculated as neutral and their stability was investigated using cohesive energy (E_{coh}), which was calculated as follows [32]:

$$E_{coh} = \frac{1}{N}\left(E_{nanocage} - xE_B - yE_N - zE_{Cu}\right) \quad (1)$$

Where $E_{nanocage}$ is the total energy of the nanocage (pure and Fe-modified); E_B, E_N and E_{Fe} are the energies of the B, N and Fe atom, respectively; x, y and z are the quantities of each atom (B, N and Fe, respectively) in the structure, and N is the total number of atoms.

The E_{ads} value for the interaction between N_2O molecules and $B_{12}N_{12}$ or Fe-$B_{12}N_{12}$ nanocages was calculated as follows:

$$E_{ads} = E_{(nanocage-N2O)} - \left(E_{(nanocage)} + E_{(N2O)}\right) + E_{BSSE} \quad (2)$$

Where $E_{(nanocage-N2O)}$ is the energy of N_2O-bonded $B_{12}N_{12}$ or Fe-$B_{12}N_{12}$ nanocage, $E_{(nanocage)}$ is the energy of pure $B_{12}N_{12}$ or Fe-modified $B_{12}N_{12}$, $E_{(N2O)}$ is the energy of the N_2O molecule, and E_{BSSE} is the basis set superposition error (BSSE).

Another important parameter for determine the possibility of the systems to be used as sensor, refers to recovery time. Such information can be obtained using the relationship between E_{ads} and the recovery time (τ) [33]:

$$\tau = v_0^{-1} e^{-E_{ads}/k_B T} \quad (3)$$

where v_0 is the attempt frequency (10^{12} s^{-1}) [34], k_B is the Boltzmann constant (8.62 x 10^{-5} eV K^{-1}), and T is the thermodynamic temperature (K).

RESULTS AND DISCUSSION

Geometry, energetic properties and stability

The optimized structures of $B_{12}N_{12}$ and Fe-modified nanocages are shown in Fig. 1 (a), and their electronic properties are presented in Table 1. The N_2O gas interaction are presented in Fig 1 (b). The results show that for $B_{12}N_{12}$ nanocage, the B-N bond lengths 1.484 and 1.437

Å are in agreement of the previous studies [21,25,35]. As seen in Fig. 1 (a), the modification with Fe atom causes a local deformation in the nanocages and this may be owing to the large radius of the doping metal atom. It is possible to observe that after optimization geometry, the Fe@b_{64} nanocage increase the B-N bond length to 2.29 Å and the Fe atom moves away from the center of the cage in the encapsuled cage. Fig. 1b shows that N_2O presents a nonlinear geometry when interacting with Fe in the decorated nanocages, binding through N atom and not through the O as preferred in other systems analyzed.

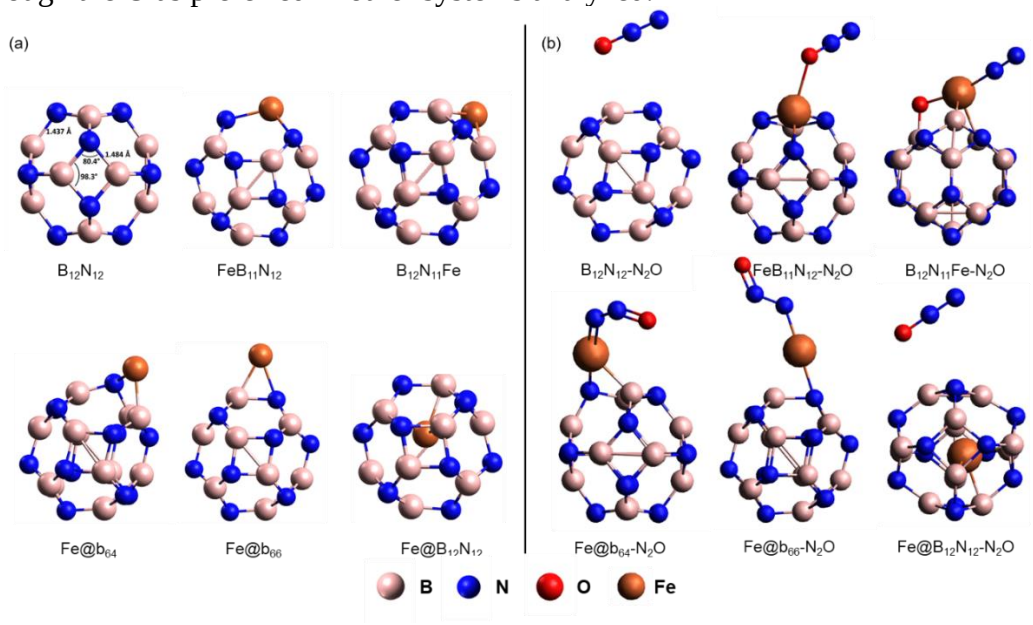

Fig. 1 – Optimized structures for pristine and Fe-modified $B_{12}N_{12}$ nanocages (a), interaction of N_2O molecule gas with isolated and Fe-modified $B_{12}N_{12}$ nanocages (b).

Table 1 shows an increase in the dipole moment (DM) of Fe-modified nanocages compared to pristine $B_{12}N_{12}$ [21,31,32], which has a none DM value due to its high symmetry. The highest DM value is observed for $B_{12}N_{11}Fe$ (DM = 4.56 Debye), which indicates a greater charge division in the nanocage, while the lowest DM value is observed for the Fe-encapsulated nanocage (DM = 0.16 Debye), which also presents the lowest charge transfer observed (-0.007 |e|), that here occurs from the cage to the Fe (negative value), unlike other systems where charge transfer is observed from the metal to the cage (positive charge), as reported by previous works [21,32,36]. Therefore, the largest charge shift from Fe to the cage is seen in the $FeB_{11}N_{12}$ system (+0.722 |e|), where the metal replaces a B atom in $B_{12}N_{12}$.

Another calculated parameter for the nanocages was the cohesion energy E_{coh}, which can be related to the systems' stability. Table 1 shows that $B_{12}N_{12}$ has a higher E_{coh} value (more negative) than Fe-modified systems, which indicates that the modified compounds are more reactive than the isolated cage [21,36], with the $FeB_{11}N_{12}$ nanocage being the second most stable of the series, with the highest value of cohesion energy (E_{coh} = -7.37 eV) and Fe@$B_{12}N_{12}$, which has the lowest value (E_{coh} = -7.11 eV), therefore, the most reactive of the series, as also observed by Silva et al. [31].

Table 1 – Electronic properties calculated: chemical hardness (η, eV), softness (S, eV^{-1}), chemical potential (μ), electrophilicity (ω / eV), dipole moment (*DM*) and the Fe atomic charges (Q, |e|).

System	*DM* / Debye	Q / |e|	E_{coh} /eV
$B_{12}N_{12}$	0.00	-	-7.40
$FeB_{11}N_{12}$	3.78	+0.722	-7.37
$B_{12}N_{11}Fe$	4.56	+0.337	-7.17
Fe@b_{64}	2.64	+0.295	-7.30
Fe@b_{66}	2.49	+0.279	-7.30
Fe@$B_{12}N_{12}$	0.16	-0.007	-7.11

N_2O adsorption analysis

Presented in Table 2 are the frontier orbitals HOMO (E_H), LUMO (E_L) and the energy gap (E_{gap}) of the isolated $B_{12}N_{12}$ and the nanocages modified with Fe, together with the energies of the HOMO, LUMO and band gap of the systems with N_2O adsorbed. Alpha and beta orbital data for open-shell systems are listed. The results show for $B_{12}N_{12}$ an E_{gap} = 6.75 eV, agreeing with results available in the literature [21,37]. However, its Fe-modification destabilizes the HOMO and stabilizes the LUMO, with an increase in the E_H values and a reduction in the E_L value of the nanocages formed. Therefore, the energy gap of the new systems is reduced in relation to the isolated cage, which causes an increase in electrical conductivity. Among the modified cages, the lowest gap is observed for Fe@b_{66} (E_{gap} = 3.24 eV (α)) and the highest E_{gap} for Fe@$B_{12}N_{12}$ (E_{gap} = 4.83 eV (α)). After N_2O adsorption, a small reduction in E_{gap} is observed for the Fe@b_{64} (α orbitals) and Fe@$B_{12}N_{12}$ (β orbitals) nanocages. While, for the other systems, the adsorption of N_2O causes an increase in the gap.

Based on the variation of E_{gap} before and after N_2O interaction, the electronic sensitivity (Δgap (%)) of the nanocage to gas adsorption is determined. The calculated Δgap (%) values indicate that the system most sensitive to N_2O gas is Fe@b_{64} (Δgap = 31.8%) and that $B_{12}N_{12}$ nanocage has low sensitivity to the gas, as also observed by Baei [26]. And this justifies the Fe-modification of $B_{12}N_{12}$ structure, which significantly improves sensitivity to N_2O.

Table 2 – The calculated values of HOMO energy (E_H), LUMO energy (E_L), energy gap (E_{gap}) and electronic sensitivity (ΔE_{gap}) between N_2O and isolated nanocages.

System	S	Isolated			With N_2O adsorbed			
		E_H (eV)	E_L (eV)	E_{gap} (eV)	E_H (eV)	E_L (eV)	E_{gap} (eV)	Δgap (%)
$B_{12}N_{12}$		-7.63	-0.75	6.88	-7.53	-0.99	6.54	4.9
$FeB_{11}N_{12}$	α	-6.72	-2.25	4.46	-6.48	-2.35	4.13	7.4
	β	-7.11	-3.70	3.41	-6.90	-3.28	3.62	6.2
$B_{12}N_{11}Fe$	α	-6.54	-2.46	4.08	-7.07	-2.72	4.35	6.7
	β	-5.36	-2.20	3.16	-6.37	-3.14	3.22	2.0
Fe@b_{64}	α	-5.06	-2.30	2.76	-5.62	-1.98	3.64	31.8
	β	-5.77	-2.20	3.57	-6.29	-2.97	3.32	6.7
Fe@b_{66}	α	-4.98	-1.74	3.24	-5.21	-1.81	3.40	5.1
	β	-5.85	-2.44	3.41	-6.02	-2.38	3.63	6.6
Fe@$B_{12}N_{12}$	α	-5.77	-0.94	4.83	-5.71	-1.06	4.66	3.6
	β	-5.06	-1.06	3.99	-4.89	-1.08	3.81	4.6

To be a good candidate as material for potential application in sensors, the nanocage needs to not only be sensitive to the desired gas, but also moderately adsorb it on own surface, so that the interaction force is not so weak, to the point of not interacting chemically with the gas, or be so intense as to retain the gas on own surface (-1 < Eads > -0.3 eV)[21,38], increasing the gas recovery time and consequently inactivating the sensor. Therefore, the adsorption energy (E_{ads}) was calculated for the systems studied after interaction with N_2O, as well as the recovery time (τ) and the results are presented in Table 3. The E_{ads} data indicate that pure $B_{12}N_{12}$ interacts very weakly with N_2O (E_{ads} = -0.14 eV), with physisorption-type interaction [26]. While Fe@$B_{12}N_{12}$ has positive adsorption energy, which implies that gas adsorption does not occur on the surface of the cage. $B_{12}N_{11}Fe$, in turn, adsorbs N_2O with very large E_{ads} for application as a sensor (E_{ads} = -5.97 eV), presenting an extremely high recovery time. The systems $FeB_{11}N_{12}$-N_2O, Fe@b_{64}-N_2O and Fe@b_{66}-N_2O present moderate E_{ads} values (E_{ads} = -

0.49, -0.70 and -0.72 eV respectively), with good recovery times (τ = 1.9 μs, 6.7 ms and 14.7 ms, respectively). Which makes them good candidates as materials for gas sensors application.

Table 3 – The calculated values of bond length Cage-N_2O (d_{BN-N2O}), adsorption energy (E_{ads}), dipole moment (DM) and Cage-N_2O bond order ($B.O.$) for interaction cage/N_2O.

System	E_{ads} / eV	τ	d_{BN-N2O} / Å	DM / Debye	Q_{CT} / |e|[a]	$B.O.$
$B_{12}N_{12}$-N_2O	-0.14	2.3 ps	2.48	0.88	+0.05	-
$FeB_{11}N_{12}$-N_2O	-0.49	1.9 μs	2.22	6.11	+2.81	0.21
$B_{12}N_{11}Fe$-N_2O	-5.97	Infinity	1.82	2.40	+2.13	0.82
Fe@b_{64}-N_2O	-0.70	6.7 ms	1.85	2.64	+2.03	0.70
Fe@b_{66}-N_2O	-0.72	14.7 ms	1.84	5.67	+1.90	0.79
Fe@$B_{12}N_{12}$-N_2O	1.16	-	2.47	1.05	- 0.07	-
N_2O	-	-	-	0.02	0.00	-

[a] Mulliken charge (The positive values indicate charge transfer from nanocages to N_2O).

The Table 3 shows that the smallest cage/N_2O distance occurs in the gas adsorption on $B_{12}N_{11}Fe$ (1.82 Å), followed by gas adsorption on Fe@b_{66} (1.85 Å) and Fe@b_{64} (1.84 Å) , while greater distances are observed for the other systems, which present B.O. very low or none. The results present that charge transfer occurs preferentially from N_2O to the cage (positive charge), the reverse occurring only in the Fe@$B_{12}N_{12}$-N_2O system. The charge transference is reflected in the cages' DM values, which are lower in systems with small charge transfer. Therefore, based on the large cage/N_2O distance, low E_{ads}, DM and B.O, it is concluded that the N_2O interaction with $B_{12}N_{12}$ and $FeB_{11}N_{12}$ and Fe@$B_{12}N_{12}$ nanocages is very weak. However, Fe@b_{64} stands out as more efficient for N_2O detecting, as it presents moderated E_{ads}, low recovery time, short cage/gas bond length (1.85 Å), with intermediate bond order (B.O. = 0.7), significant charge transfer and best sensitivity to N_2O in the series (Δgap = 32%).

CONCLUSIONS

DFT-D3 level calculations with B3LYP functional and 6-31G(d,p) basis set have been employed in this work for exploring the geometrical and energetical properties of N_2O-adsorbed on bare and Fe-modified $B_{12}N_{12}$ nanocages. The results indicate the N_2O gas is physically adsorbed (E_{ads} > -0.3 eV) on pristine $B_{12}N_{12}$, $FeB_{11}N_{12}$, $B_{12}N_{11}Fe$, Fe@b_{66} and Fe@$B_{12}N_{12}$ nanocages, by weak interaction. But, the N_2O gas is chemically adsorbed by stronger interaction in Fe@b_{64} nanocage (E_{ads} = 0.70 eV). Thus, Fe@b_{64}–N_2O system shown a moderate interaction and a good recovery time (τ = 6.7 ms). Furthermore, the Fe@b_{64} electronic sensitivity (ΔE_{gap} = 32 %) toward N_2O molecule is the best compared with other modified systems. In summary, according our computational results for energy gap, it was considered that Fe@b_{64} nanocage can be employed as material for conductometric type sensor for N_2O molecule gas determination.

ACKNOWLEDGMENTS

The authors acknowledge the financial support provided by CAPES, CNPq, and FAPEMA.

REFERENCES

[1] DEKSNYS, T. P.; MENEZES, R.R.; FAGURY-NETO, E.; KIMINAMI, R.H.G.A. Synthesizing Al_2O_3/SiC in a microwave oven: a study of process parameters. Ceram. Int., v. 33, n. 1, p. 67-71, 2007.

[2] X. ZHOU; W.Q. TIAN; X.-L. WANG; Adsorption sensitivity of Pd-doped SWCNTs to small gas molecules, Sensors Actuators, B: Chemical. v. 151, n. 1, p. 56–64, 2010.

[3] Z.M. AO; J. YANG; S. LI; Q. JIANG. Enhancement of CO detection in Al doped graphene, Chem. Phys. Lett. v. 46, n. 4-6, p. 276–279, 2008.

[4] M. PYKAL; P. JURE˘CKA; F. KARLICKÝ; M. OTYEPKA. Modelling of graphene functionalization, PCCP v. 18, n. 9, p. 6351–6372, 2016.

[5] O. LEENAERTS; B. PARTOENS, F.M. PEETERS, Adsorption of H_2O, NH_3, CO, NO_2, and NO on graphene: A first-principles study, Phys. Rev. B - Condensed Matter Mater. Phys. v. 77, 2008.

[6] Y.-H. ZHANG; Y.-B. CHEN; K.-G. ZHOU; C.-H. LIU; J. ZENG; H.-L. ZHANG; Y. PENG. Improving gas sensing properties of graphene by introducing dopants and defects: A first-principles study, Nanotechnology. v. 20, n. 18, 185504 (2009).

[7] J. DAI; J. YUAN; P. GIANNOZZI. Gas adsorption on graphene doped with B, N, Al, and S: A theoretical study, Appl. Phys. Lett. v. 95, n. 23, 232105 (2009).

[8] SHETTIA, N.P.; MISHRA, A.; BASU, S.; AMINABHAVI, TM. Versatile fullerenes as sensor materials. Mater. Today Chem v. 20, 100454 (2021).

[9] CHUANG, C-W; SHIH, J-S. Preparation and application of immobilized C_{60}-glucose oxidase enzyme in fullerene C_{60}-coated piezoelectric quartz crystal glucose sensor. Sensors and Actuators B v. 81, p. 1–8, 2001.

[10] KESHTKAR S.; RASHIDI A.; KOOTI M.; ASKARIEH M.; POURHASHEM S.; GHASEMY E.; IZADI N. A novel highly sensitive and selective H_2S gas sensor at low temperatures based on SnO_2 quantum dots-C_{60} nanohybrid: experimental and theory study. Talanta v. 188, p. 531–539, 2018.

[11] PAINE R.T.; NARULA C.K. Synthetic routes to boron nitride. Chem. Rev. v. 90, p. 73–91, 1990.

[12] OKU T.; HIRANO T.; KUNO M.; KUSUNOSE T.; NIIHARE K.; SUGANUMA K. Synthesis, atomic structures and properties of carbon and boron nitride fullerene materials. Mater. Sci. Eng. B v. 74, p. 206–217, 2000.

[13] G. SEIFERT; R. FOWLER; D. MITCHELL; D. POREZAG; AND T. FRAUENHEIM Chem. Phys. Lett. v. 268, p. 352–358, 1997.

[14] OKU T.; NISHIWAKI A.; NARITA I. Formation and atomic structure of $B_{12}N_{12}$ nanocage clusters studied by mass spectrometry and cluster calculation. Sci. Technol. Adv. Mater. v. 5, p. 635−645, 2004.

[15] RAD A.S.; AYUB K. Enhancement in hydrogen molecule adsorption on $B_{12}N_{12}$ nano-cluster by decoration of nickel. Int J Hydrog Energy v. 41, p. 22182–22191, 2016.

[16] RAHIMI F.; ZABARADSTI A. Photo-Induced Electron Transfer Process on Pristine and Sc-Substituted $B_{12}N_{12}$ Nanocage as H_2S Chemosensor: A Fully DFT and TD-DFT Study. J Inorg Organomet Polym v. 27, p. 1770–1777, 2017.

[17] HUSSAIN S.; HUSSAIN R.; MEHBOOB M.Y., CHATHA S.A.S.; HUSSAIN A.I.; UMAR A.; KHAN M.U.; AHMED M.; ADNAN M.; AYUB K. Adsorption of Phosgene Gas on Pristine and Copper-Decorated $B_{12}N_{12}$ Nanocages: A Comparative DFT Study. ACS Omega v. 5, p. 7641–7650, 2020.

[18] SILVA A.L.P., SOUSA N.S., VARELA JÚNIOR J.J.G. Theoretical studies with $B_{12}N_{12}$ as a toxic gas sensor: a review. J. Nanoparticle Res. v. 25, n. 22, 2023.

[19] AMMAR H.Y.; BADRAN H.M.; EID K.H.M. TM-doped $B_{12}N_{12}$ nano-cage (TM = Mn, Fe) as a sensor for CO, NO, and NH_3 gases: A DFT and TD-DFT study. Mater Today Commun v. 25, 101681 (2020).

[20] BEHESHTIAN J.; BAGHERI Z.; KAMFIROOZI M.; AHMADI A. Toxic CO detection by $B_{12}N_{12}$ nanocluster. Microelectronics J v. 42, p. 1400–1403, 2011.

[21] SILVA A.L.P.; VARELA JÚNIOR, J.J.G. Carbon monoxide interaction with $B_{12}N_{12}$ nanocage with and without an external electric field: a DFT study. J Nanopart Res v. 24, n. 1, 2022.

[22] CUI H.; JIA P.; PENG X.; LI P. Adsorption and sensing of NO and C_2H_2 by S-defected SnS_2 monolayer for DGA in transformer oil: A DFT study. Mater. Chem. Phys. v. 249, 123006 (2020).

[23] HOSSAIN M.D.A.; HOSSAIN M.D.R.; HOSSAIN M.D.K.; KHANDAKER J.I.; AHMED F.; FERDOUS T.; HOSSAIN M.D.A. An ab initio study of the B_{35} boron nanocluster for application as atmospheric gas (NO, NO_2, N_2O, NH_3) sensor. Chem. Phys. Lett. v. 754, 137701 (2020).
[24] BAEI M.T. Si-Doped $B_{12}N_{12}$ Nanocage as an Adsorbent for Dissociation of N_2O to N_2 Molecule. Heteroat. Chem. v. 24, p. 476–481, 2013.
[25] A. SHOKUHI RAD; AND K. AYUB, O_3 and SO_2 sensing concept on extended surface of $B_{12}N_{12}$ nanocages modified by Nickel decoration: A comprehensive DFT study. Solid State Sci. v. 69, p. 22–30, 2017.
[26] ROSTAMOGHLI, R., VAKILI, M., BANAEI, A., POURBASHEER, E., & JALALIERAD, K. Applying the B12N12 nanoparticle as the CO, CO2, H2O and NH3 sensor. *Chemical Review and Letters*, *1*(1), p. 31-36, 2018.
[27] NEESE F. Software update: the ORCA program system, version 4.0. WIREs Comput. Mol. Sci. v. 8, n. 1327, 2018.
[28] GRIMME S. Semiempirical GGA-type density functional constructed with a long-range dispersion correction. J. Comp. Chem. v. 27, p. 1787–1799, 2006.
[29] SILVA A.L.P.; VARELA JÚNIOR JJG (2023) Density Functional Theory Study of Cu-Modified $B_{12}N_{12}$ Nanocage as a Chemical Sensor for Carbon Monoxide Gas. Inorg. Chem. v. 62, p. 1926–1934, 2023.
[30] HOSSAIN M.D.R.; HASAN M.D.M.; NISHAT M.; NOOR-E-ASHRAFI; AHMED F.; FERDOUS T.; HOSSAIN M.D.A. DFT and QTAIM investigations of the adsorption of chlormethine anticancer drug on the exterior surface of pristine and transition metal functionalized boron nitride fullerene. J. Mol. Liq. v. 323, 114627 (2021).
[31] KOETTGEN J.; ZACHERLE T.; GRIESHAMMER S.; MARTIN M. Ab initio calculation of the attempt frequency of oxygen diffusion in pure and samarium doped ceria. *Phys. Chem. Chem. Phys*. v. 19, p. 9957-9973, 2017.
[32] KAEWMARAYA T.; NGAMWONGWAN L.; MOONTRAGOON P.; JARERNBOON W.; SINGH D.; AHUJA R.; KARTON A.; HUSSAIN T. Novel green phosphorene as a superior chemical gas sensing material. *J. Hazard. Mater*. v. 401, 123340 (2021).
[33] H.M. BADRAN, KH.M. EID, H.Y. AMMAR, A DFT study on the effect of the external electric field on ammonia interaction with boron nitride nano-cage, Journal of Physics and Chemistry of Solids v. 141, 109399 (2020).
[34] ABBASI M.; NEMATI-KANDE E.; DOUST MOHAMMADI M.; Doping of the firstrow transition metals onto B12N12 nanocage: a DFT study, Comput. Theor. Chem. v. 1132, p. 1–11, 2018.
[35] S. LARKI; E. SHAKERZADEH; E.C. ANOTA; R. BEHJATMANESH-ARDAKANI The Al, Ga and Sc dopants effect on the adsorption performance of $B_{12}N_{12}$ nanocluster toward nictogen hydrides, Chemical Physics v. 526, 110424 (2019).
[36] FAN G.; WANG X; TU X.; XU H.; WANG Q.; CHU X. Density functional theory study of Cu-doped BNNT as highly sensitive and selective gas sensor for carbon monoxide. *Nanotechnology*. v. 32, 075502 (2021).
[37] Grimme S (2011) Density functional theory with London dispersion corrections. WIREs Comput. Mol. Sci. 1:211–228.
[38] Cui H, Zhang X, Zhang G, Tang J (2019) Pd-doped MoS2 monolayer: a promising candidate for DGA in transformer oil based on DFT method. Appl. Surf. Sci. 470:1035–1042.